A Comparative ^{13}C NMR Study of Local Ordering in a Homologous Series of Bent-core Liquid Crystals

Ronald Y. Dong*

Department of Physics and Astronomy, University of British Columbia, Vancouber, BC, Canada V6T 1Z1

Received: November 1, 2008; Revised Manuscript Received: December 12, 2008

A ^{13}C NMR study is carried out in a number of banana-shaped molecules belonging to a homologous series. The derivatives contain chlorine or bromine substituent(s) in the center ring of 1,3-phenylene bis[4′-alkenyloxy biphenyl]-4-carboxylate (nPBBC), and different terminal chain lengths are systematically compared in terms of their local order parameters and their ability to form an aligned nematic phase in the NMR magnet. The chemical shift anisotropy tensors measured from nPBBC by fitting the ^{13}C powder patterns are now extensively used on these molecules to interpret their observed ^{13}C chemical shifts in the nematic phase. The bend angles are estimated as a function of temperature in two members of the nPBBC series. Conformation twists in the bent-core region inferred from the local molecular biaxial paramters are discussed.

1. Introduction

Since the discovery of liquid crystals (LC) formed from bent-core molecules,[1] they have received much interest because of the associated new class of "banana" (B) phases that show potential technical relevance, and also of the long sought for biaxial nematic phase in thermotropic LC systems. This new classs of molecules possesses a V-shaped structure (usually a five aromatic rings system in the "rigid" core with terminal chains), thereby exhibiting the necessary molecular biaxiality required in the prediction of biaxial nematics by Freiser.[2] Another novel property of this class of materials is the formation of tilted layer structures in various B_1-B_7 phases. Although these V-shaped molecules are achiral, because of the effective packing and polarity they can show chirality and become switchable electro-optically.[3] Nuclear magnetic resonance (NMR) spectroscopy has played a dominant role in characterizing orientational order parameters in uniaxial and biaxial mesophases of LC.[4−7] In terms of an order supermatrix $S^{ii}_{\nu\mu}$, where $i = (X, Y, Z)$ refers to the principal axis of the laboratory (L) frame, and $\nu,\mu = (x, y, z)$ denote an axis of the molecular (M) frame attached on the molecule, four common order parameters in the simple case (e.g., biaxial nematic) are:[8]

$$S = S^{ZZ}_{zz}, \quad D = S^{ZZ}_{xx} - S^{ZZ}_{yy}, \quad P = S^{XX}_{zz} - S^{YY}_{zz}, \quad C = \left(S^{XX}_{xx} - S^{XX}_{yy}\right) - \left(S^{YY}_{xx} - S^{YY}_{yy}\right)$$

The order parameters S and D are nonzero, whereas P and C are zero in the uniaxial nematic (N) phase (for a cylindrical rod, D is also identical to zero); in the biaxial nematic phase all four order parameters are nonzero. It is interesting to note the evidence of similar temperature behaviours for D and C observed in the biaxial nematic phase of tetrapode molecules.[9] In general, there exist more orientational order paramters (see next section) depending on the symmetry of the phase and the symmetry of the LC forming molecules. One structural factor of V-shaped molecules is the bend angle Θ subtended by the two lateral wings next to the central ring (see Figure 1a). The phase diagrams predicting the presence of biaxial nematic phase and the uniaxial−biaxial nematic phase transition seem to depend on the magnitude of the bend angle.[10,11] A Θ angle approaching 110° is most favored to induce a biaxial nematic phase. Apart from the ability to study local order parameters of various fragments in the bent-core, NMR can also shed light on the average molecular structure and provides a means to estimate the bend angle in V-shaped molecules. It has recently been pointed out that local order matrices for para (p) axes of phenyl rings may be better than the principal order parameters of the V-shaped molecule to study the onset of phase biaxiality, i.e., S^{XX}_{pp} differs from S^{YY}_{pp} in simulation. [12] For this reason, ^{13}C NMR is indispensable for examining site-specific information, specifically regarding local order parameters, and has been adopted to study biaxial nematic phases when deuterated materials are unavailable. [13] It is noted that one of our earlier works on the homologous nPBBC series (1,3-phenylene bis[4′-alkenyloxy biphenyl]-4-carboxylate derivatives) has instead aimed at determining the order parameter S of the molecular core, while ignoring the molecular biaxiality as a first approximation. [14] In fact, local fragment biaxiality could play an essential role in shedding light on conformations within the aromatic region of the V-shaped molecules.

The homologous nPBBC series has been studied using ^{13}C NMR chemical shifts, $\langle\delta\rangle$, in the uniaxial nematic (N) phase as well as using a two-dimensional NMR technique termed as separation of undistorted powder patterns by effortless recoupling (SUPER) in a rotating solid sample at the magic angle[15] to determine the chemical shift anisotropy (CSA) tensors of various carbons in the past.[14,16,17] The lack of suitable CSA tensors have prevented us in an earlier report[14] to do an in-depth and self-consistent analysis of the observed $\langle\delta\rangle$ values in the nPBBC series. Indeed the derived order parameters and the bend angle based on $\langle\delta\rangle$ relative to its corresponding isotropic shift may be problematic unless the principal components and the orientation of each CSA tensor are known. Recently we found that density functional theory (DFT) can indeed be useful for calculating CSA tensors to compare with those obtained by the SUPER method.[18] Furthermore, the orientation of the CSA tensor in the molecular frame can be directly obtained in DFT calculations. Such information is lacking in the SUPER method, as it can only provide the CSA powder patterns. The present report aims to provide new ^{13}C analyses of four molecules—

* E-mail: rondong@phas.ubc.ca.

10.1021/jp8096692 CCC: $40.75
Published on Web 01/22/2009

10DClPBBC, 11ClPBBC, 10ClPBBC, and 10BrPBBC (Figure 1a)—using their own CSA tensors and previous experimental data reported in the literature. In particular, the local order parameter tensors of various fragments in each mesogen are exploited in order to contrast their molecular conformations in the bent-core region as well as their different field alignment effects. The paper is organized as follows. A brief review of the theory of chemical shift interaction in the mesophase is given in the next section. This is followed by the section on Results and Discussion. A brief summary is given at the end.

2. Theory

To allow the discussion of ^{13}C chemical shifts, $\langle\delta\rangle$, in the mesophase, only the necessary formulas are given here, and the details can be found in the literature.[19] The time-averaged chemical shift Hamiltonian in the high-field limit is given by eq 1,

$$\bar{H}_{CS} = \gamma\hbar B I_z \delta_{iso} + \sqrt{\frac{2}{3}}\gamma\hbar B I_z \langle R_{2,0}\rangle \tag{1}$$

where the bar over the Hamiltonian denotes a time average over internal bond rotations and overall motions of the molecule, and $\langle R_{2,0}\rangle$ is the corresponding time-averaged second rank irreducible spherical tensor in the L frame. To describe internal motions of the fragment and overall motions of the molecules, the following Euler transformations need to be considered, as illustrated in Figure 1b:

$$\text{L frame } (\vec{B}) \overset{(\varphi_0,\,\theta_0,\,\psi_0)}{\varphi} \text{ Director frame } (\vec{n})$$

$$\text{Director frame } (\vec{n}) \overset{(\varphi,\,\theta,\,\psi)}{\Rightarrow} \text{Molecular frame } (x,y,z)$$

$$\text{Molecular frame } (x,y,z) \overset{(\alpha_F,\,\beta_F,\,\gamma_F)}{\varphi} \text{ Fragment frame } (x',y',z')$$

$$\text{Fragment frame } (x',y',z') \overset{(0,\,\beta_P,\,\pi/2)}{\Rightarrow} \text{PAS frame } (\delta_{11},\,\delta_{22},\,\delta_{33})$$

The transformation from the fragment frame (x', y', z') to PAS frame (δ_{11}, δ_{22}, δ_{33}) involves $\beta_P = 60°$, 120° for protonated carbons, and $\beta_P = 0°$ for quaternary carbons, and the Euler angles (α_F, β_F, γ_F) are those to transform between the M and fragment frame. Now, the observed chemical shift of a particular carbon site in a mesophase can be calculated:[19]

$$\begin{aligned}\langle\delta\rangle &= \delta_{iso} + \sqrt{\frac{2}{3}}\langle R_{2,0}\rangle \\ &= \delta_{iso} + a\left(\sqrt{\frac{2}{3}}P_2(\cos\beta_F)R'_{2,0} + (\sin^2\beta_F)R'_{2,2}\right) + \\ &\quad b\left(\sqrt{\frac{3}{8}}(\sin 2\beta_F)R'_{2,0} - \frac{1}{2}(\sin 2\beta_F)R'_{2,2}\right) + \\ &\quad c\left(\sqrt{\frac{3}{8}}(\sin^2\beta_F)R'_{2,0} + \frac{1}{2}(1+\cos^2\beta_F)R'_{2,2}\right)\end{aligned} \tag{2}$$

where the primed tensor $R'_{2,n}$ in the fragment frame (x', y', z') are given by:

$$\begin{aligned}R'_{2,0} &= \sqrt{\frac{2}{3}}\left[P_2(\cos\beta_P)(\delta_{33}-\delta_{22}) + \frac{1}{2}(\delta_{22}-\delta_{11})\right] \\ R'_{2,\pm1} &= \mp\frac{1}{2}\sin 2\beta_P(\delta_{33}-\delta_{22}) \\ R'_{2,\pm2} &= \frac{1}{2}[(\sin^2\beta_P)\delta_{33} + (\cos^2\beta_P)\delta_{22} - \delta_{11}]\end{aligned} \tag{3}$$

and

$$\begin{aligned}a &= P_2(\cos\theta_0)S_{00} + \frac{3}{4}\sin 2\theta_0 \sin\varphi_0 S_{10} + \frac{3}{4}\sin^2\theta_0 \cos 2\varphi_0 S_{20} \\ b &= P_2(\cos\theta_0)S_{01} + \sin 2\theta_0 \sin\varphi_0 S_{11} - \sin^2\theta_0 \cos 2\varphi_0 S_{21} \\ c &= -P_2(\cos\theta_0)S_{02} + \sin 2\theta_0 \sin\varphi_0 S_{12} - \sin^2\theta_0 \cos 2\varphi_0 S_{22}\end{aligned} \tag{4}$$

are coefficients involving the nine generalized order parameters: molecular order parameters $S_{00} = S_{zz}^{ZZ} \equiv S$, $S_{01} = (4/3)S_{yz}^{ZZ}$, and $S_{02} = (2/3)(S_{xx}^{ZZ} - S_{yy}^{ZZ}) \equiv (2/3)D$, as well as six phase biaxial order parameters:[20]

$$\begin{aligned}S_{10} &= \langle\sin 2\theta \sin\varphi\rangle \\ S_{11} &= \langle\cos\theta\cos\varphi\cos\psi - \cos 2\theta \sin\varphi \sin\psi\rangle \\ S_{12} &= \left\langle\sin\theta\cos\varphi\sin 2\psi + \frac{1}{2}\sin 2\theta \sin\varphi\cos 2\psi\right\rangle \\ S_{20} &= \langle\sin^2\theta\cos(2\varphi)\rangle = \frac{2}{3}P \\ S_{21} &= \left\langle\sin\theta\sin 2\varphi\cos\psi + \frac{1}{2}\sin 2\theta\cos 2\varphi\sin\psi\right\rangle \\ S_{22} &= \frac{1}{2}\langle(1+\cos^2\theta)\cos 2\varphi\cos 2\psi - \\ &\quad 2\cos\theta\sin 2\varphi\sin 2\psi\rangle = \frac{1}{3}C\end{aligned} \tag{5}$$

Now, the phase biaxial order parameters appear always multiplying by either $\sin 2\theta_0$ or $\sin\theta_0$ in the coefficients a, b, c of eq 4. Thus, they become unobservable when $\theta_0 = 0$, which is normally the case for an aligned sample with the director lying along the external magnetic field. As a consequence, the phase biaxiality is usually not needed in interpreting ^{13}C chemical shifts in aligned mesophases. For a uniaxial phase, eq 2 reduces to:

$$\begin{aligned}\langle\delta\rangle = \delta_{iso} + \sqrt{\frac{2}{3}}P_2(\cos\theta_0) \times \Bigg\{&\left[P_2(\cos\beta_F)S_{00} + \frac{3}{4}\sin(2\beta_F)S_{01} - \frac{3}{4}\sin^2\beta_F S_{02}\right]R'_{2,0} + \\ &\left[\sqrt{\frac{3}{2}}\sin^2\beta_F S_{00} - \sqrt{\frac{3}{8}}\sin(2\beta_F)S_{01} - \sqrt{\frac{3}{8}}(1+\cos^2\beta_F)S_{02}\right]R'_{2,2}\Bigg\}\end{aligned} \tag{6}$$

Note that the observed chemical shift $\langle\delta\rangle$ is still scaled by the second Legendre $P_2(\cos\theta_0)$ should the director not be along the magnetic field.

If molecules have fast rotations about their long axes, such as in uniaxial N and Sm*A* phases, S_{01} is averaged to zero, and for the director aligned along the magnetic field ($\theta_0 = 0$), eq 6 then becomes:

$$\langle\delta\rangle = \delta_{iso} + \left(\sqrt{\frac{2}{3}}P_2(\cos\beta_F)R'_{2,0} + (\sin^2\beta_F)R'_{2,2}\right)S - \frac{2}{3}\left(\sqrt{\frac{3}{8}}(\sin^2\beta_F)R'_{2,0} + \frac{1}{2}(1+\cos^2\beta_F)R'_{2,2}\right)D \quad (7)$$

By setting β_F to 0, the segmental order parameters S' (or S'_{00}) and D' (or S'_{02}) can be obtained from

$$\langle\delta\rangle = \delta_{iso} + \frac{2}{3}S'\left[P_2(\cos\beta_P)(\delta_{33}-\delta_{22}) + \frac{1}{2}(\delta_{22}-\delta_{11})\right] + \frac{1}{3}D'[\delta_{11} - \delta_{22}\cos^2\beta_P - \delta_{33}\sin^2\beta_P] \quad (8)$$

Thus, we can get the local molecular order parameters S' and D' for the biphenyl fragment and the phenyl ring by fitting the observed ^{13}C chemical shifts from each fragment. By comparing eqs 7 and 8, the relation:[22]

$$S' \approx SP_2(\cos\beta_F) \quad (9)$$

is found, which allows the determination of the β_F angle. In the following, the superscripts on the local ordering S' and D' will be omitted for simplicity, with the understanding that they refer to local ordering of each aromatic fragment.

3. Results and Discussion

A typical set of ^{13}C spectra for the 10DClPBBC sample is shown in Figure 2a, and the phase sequences of the nPBBC series studied here are schematized in Figure 2b.

3.1. 10DClPBBC. The temperature-dependent $\langle\delta\rangle$ for the aromatic region and X9 and X10 in the N phase of 4,6-dichloro-1,3-phenylene bis[4′-(9-decenyloxy)-1,1′-biphenyl] carboxylate (10DClPBBC)[16] are reproduced in Figure 3. At the I−N transition, ^{13}C $\langle\delta\rangle$ of the aromatic carbons shift markedly downfield, but those of the aliphatic carbons shift slightly upfield. Because aliphatic carbon peaks are often overlapped (as in this case except for X9 and X10), the aromatic carbons are investigated in detail to extract both the local orientational order parameters of the bent-core and its "average" molecular structure.

The ^{13}C $\langle\delta\rangle$ in a N phase is related to its isotropic δ_{iso} value by eq 8. To fit the observed $\langle\delta\rangle$ values in the N phase, the CSA values measured by SUPER in 10DClPBBC and in 10ClPBBC as listed in Tables 1 and 2, respectively, together with the principal CSA components (ppm) for C2 (8.7, 135.5, 192.9)[23] are used. It is important to point out the CSA tensors listed in ref 17 must be corrected as done in Table 2, since their results had unfortunately missed a scaling factor of 0.667 for the isotropic shifts. This table is used for those carbon sites whose CSA tensors were unavailable in the SUPER experiment of 10DClPBBC. Besides the determination of CSA tensors in 10ClPBBC, the sample was found not to align by cooling in a magnetic field of 9.4T from the I phase. Now, the CSA tensor's PAS (1, 2, 3) is chosen by assuming that its 3 axis is along a C−H bond, or C−C bond (along the para axis direction), with the 1 axis normal to a ring plane (see Figure 1b). The assumption appears to be reasonable as the orientation of the CSA tensor for various carbons have been compared with those derived from DFT calculations.[18] In using eq 8, $\beta_P = 0$ for quaternary carbons (carbon 1, 4, 5, 8) and $\beta_P = 60°$ for protoned carbons (carbon 2, 3, 6, 7) on the biphenyl groups are used, whereas $\beta_P = 90°$ for C12 and $\beta_P = 150°$ for C10 on the central ring. D values were found to depend linearly on temperature. To globally analyze the chemical shifts, one can use the Haller equation for S, viz. $S(T) = S_0(1 - T/T^*)^f$, where S_0 and f are empirical

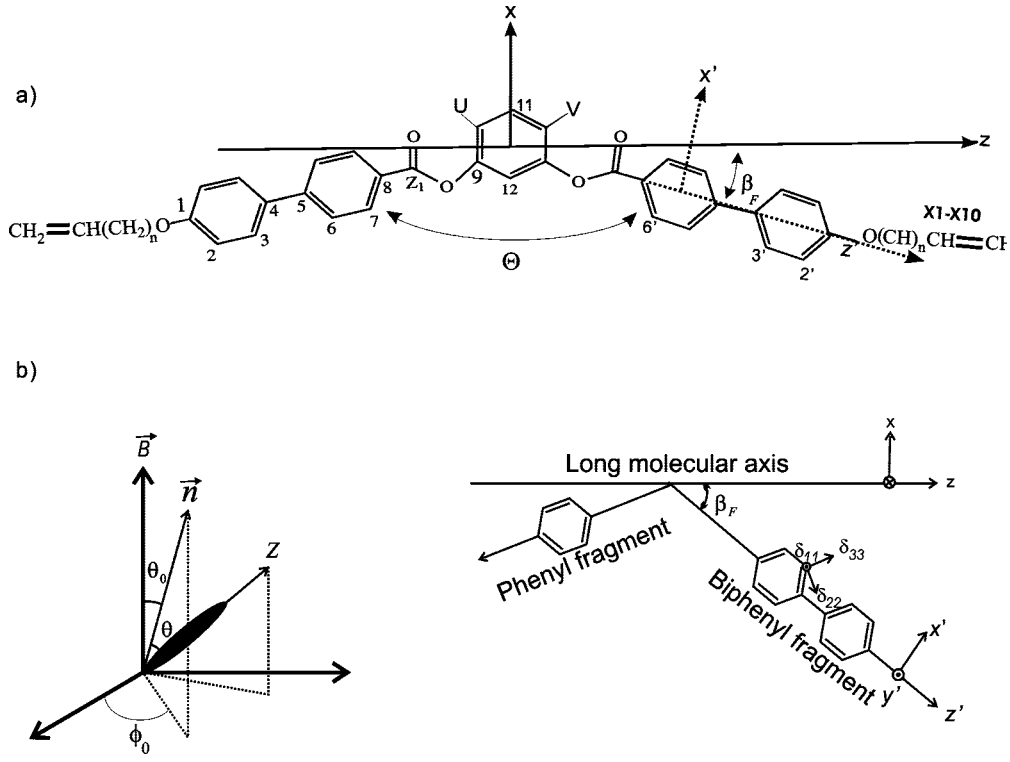

Figure 1. (a) Molecular structure of nPBBC LC: 10DClPBBC (n = 10, U = V = Cl), 11ClPBBC (n = 11, U = Cl, V = H), 10ClPBBC (n = 10, U = Cl, V = H), 10BrPBBC (n = 10, U = Br, V = H); when U = V, the primed carbon labels become unprimed. (b) Schematic of the orientation of a molecule with respect to the director n in the magnetic field ($\vec{B}$), and schematic of a CSA (δ_{11}, δ_{22}, δ_{33}) PAS frame, a fragment (x', y', z'), and a molecular frame (x, y, z) fixed on the molecule.

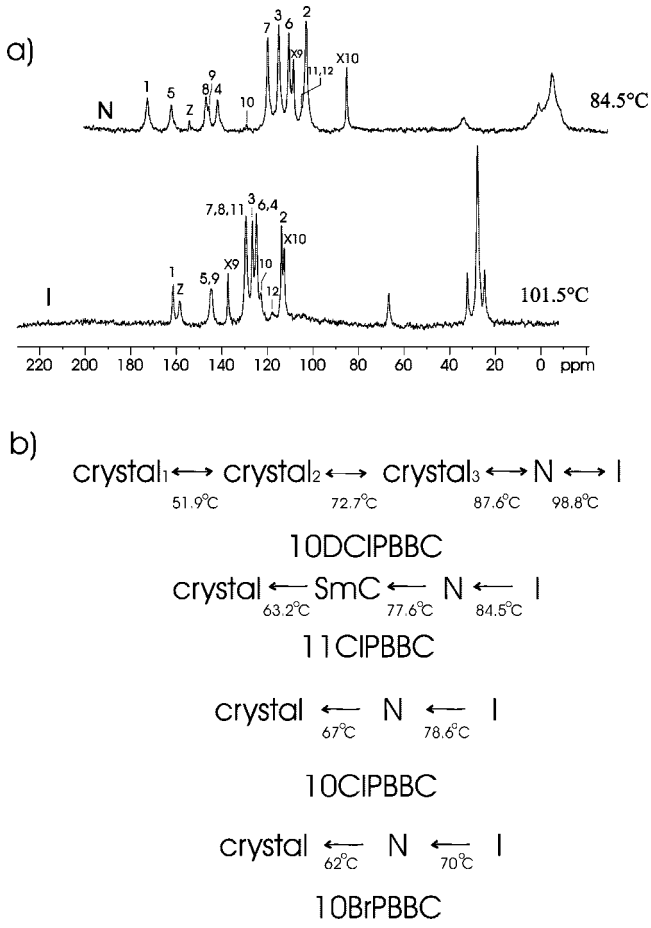

Figure 2. (a) Typical ^{13}C NMR spectra of 10DClPBBC in the isotropic and nematic phase. (b) Phase sequences of the studied nPBBC LC.

constants, and T^* ($T^* = T_c + 1$ K) is the temperature slightly above T_c at which $S_{z'z'}$ vanishes. Also, a linear equation has been used to describe the temperature dependence of D, that is, $D = \Delta(T - T_c)$ where Δ was a fitting constant.

The local order parameters for all the phenyl rings are, therefore, obtained by optimizing the fittings between the calculated and experimental $\langle\delta\rangle$, and the calculated $\langle\delta\rangle$ values are shown as solid lines in Figure 3. The derived local S values of the central ring and biphenyl groups are shown in Figure 4 with S_0 and f for the biphenyl group and central ring being given by (0.698, 0.159) and (0.858, 0.137), respectively. Figure 4 also shows the linear temperature behaviours of the D for the two biphenyl rings and central ring. These results imply that the local z-axis located on the central ring represents a more ordered axis (or the long molecular axis), and thus reflects the overall molecular ordering. The z'-axis along the para axes in the biphenyl group is less ordered. Now one can relate the ordering of these local z-axes using eq 9, where β_F is the angle between the para axes of the biphenyl group and the more ordered axis (z-axis of the center ring). Using this equation, the β_F angle is found to vary with temperature, increasing from 26 to 29° upon decreasing temperature. Hence, the bend angle Θ subtended by the two lateral arms in 10DClPBBC is also temperature dependent, ranging between 128 and 122° at the low temperature end (see Figure 5). It is noted that among all the phenyl rings, the D value for the inner ring in the biphenyl group and the center ring have similar magnitude, but their signs are opposite. Thus, these two phenyl ring planes oriented differently with respect to the director, implying a definite twist conformation in the molecular core. Also, a slight twist of the phenyl ring

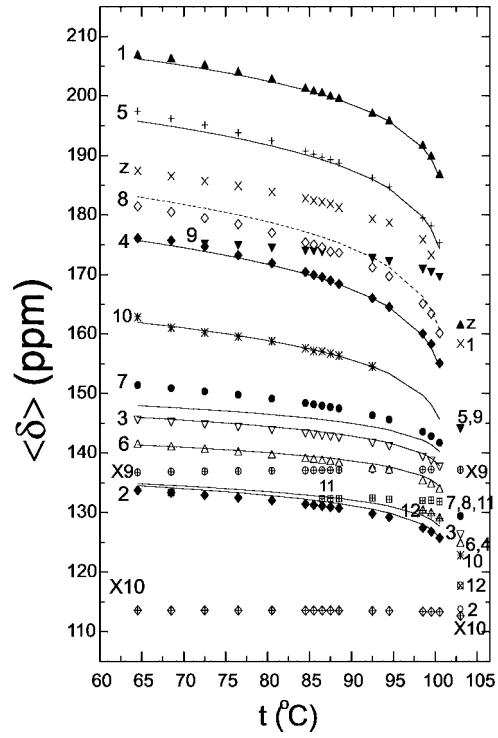

Figure 3. Plots of $\langle\delta\rangle$ for the aromatic carbons and aliphatic carbons X9 and X10 in the isotropic and nematic phases of 10DClPBBC. The carbon labels are those indicated in Figure 1. Solid curves denote calculated $\langle\delta\rangle$ values after a global minimization.

TABLE 1: CSA Tensors for Various Carbon Sites of 10DClPBBC (Carbon Labels Same for Both Lateral Wings)[a]

sites	6	7	9	10	12	z
δ_{11}	34.4	28.3	72.2	44.6	30	111
δ_{22}	140.7	145.7	145.2	109	149.3	133
δ_{33}	204.6	212.7	217.2	213.6	183	242

[a] Determined from SUPER with an Uncertainty in Each Principal Value of ca ± 3 ppm.

TABLE 2: CSA Tensors for Carbons Obtained from SUPER in 10ClPBBC[a]

sites	1	3	4	5	7
δ_{11}	50.4	9.6	27.3	58.9	11.3
δ_{22}	161.2	146.8	127.4	129.9	154.5
δ_{33}	257.2	216.5	223.7	249.3	219.7
sites	8	9	11	13	14
δ_{11}	8.6	44.6	29.3	44.6	30.7
δ_{22}	144.9	160.1	130.7	160.1	124.2
δ_{33}	229.0	261.8	201.7	261.8	189.6

[a] Principal values from ref 17 are corrected for the missing scaling using $\delta_{ii}^{new} = (\delta_{ii} - \delta_{iso})/0.667 + \delta_{iso}$.

planes in the biphenyl fragment can be inferred from Figure 4. For the center ring, D is about 0.01 at 64.5 °C and vanishes at T_c.

The present analysis does not require specific motional processes (internal and external motions of the bent-core) or need to know its particular core conformation. Indeed, there may be several possible configurations generated by a rotation of the lateral arm about the $C_{ar}-O$ bond at the central ring.[16] Note that the conformational changes must be fast on the NMR time scale as only one ^{13}C spectrum is observed at a particular temperature. Otherwise, different subspectra would be visible

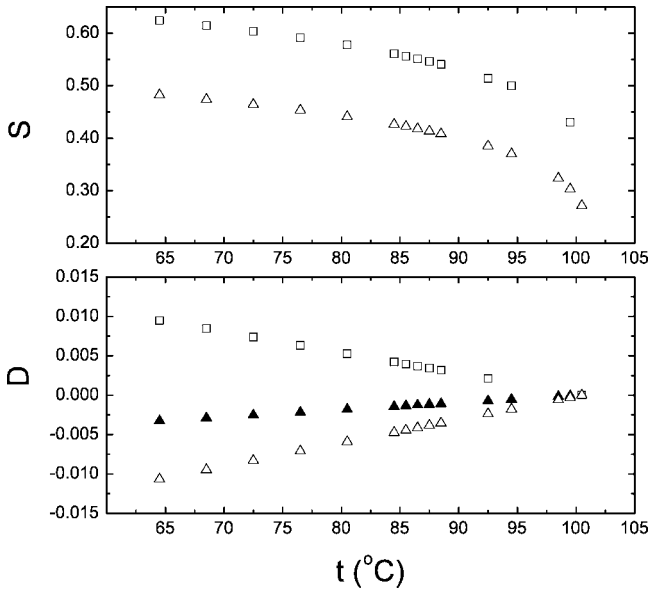

Figure 4. Top: Plot of the local order parameter S for the biphenyl group (triangles) and central ring (squares) in the N phase of 10DClPBBC. Bottom: Plot of the local biaxial order parameter D vs temperature for the center ring (squares), and in the biphenyl group for the ring closer to the center ring (triangles), and for the outer ring (full triangles).

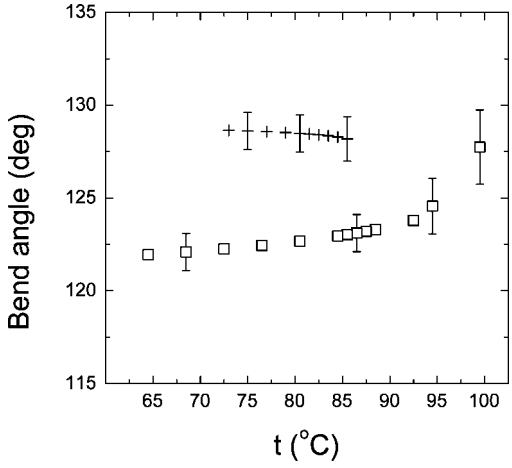

Figure 5. Plot of the bend angle versus temperature in the uniaxial nematic phase of 10DClPBBC (squares) and of 11ClPBBC (pluses).

in the observed spectrum just like the doubling of the ^{13}C peaks seen in a monosubstituted homologue 11ClPBBC.[14] Finally, the bend angle Θ may be interpreted as some configurational average angle between the two lateral wings in this bent-core molecule. The question of exactly how many (if any) conformations and their structures as well as their probabilities for a relatively large molecule remains open. Indeed, DFT calculations of different configurations in the energy surface landscape may be a first step to possibly address the conformation states in the bent-core region.

3.2. 11ClPBBC. The same approach used to treat 10DClPBBC can be applied to analyze the chemical shift data observed in the N phase of 4,6-chloro-1,3-phenylene bis[4′-(10-undecenyloxy)-1,1′-biphenyl] carboxylate (11ClPBBC). The temperature-dependent $\langle\delta\rangle$ for the aromatic region and X10 and X11 of 11ClPBBC[14] are reproduced in Figure 6. Notice the fact that 11ClPBBC has a monosubstituted chlorine on the central ring; the two biphenyl fragments become inequivalent to generate two subspectra of aromatic carbon peaks. The same set of CSA

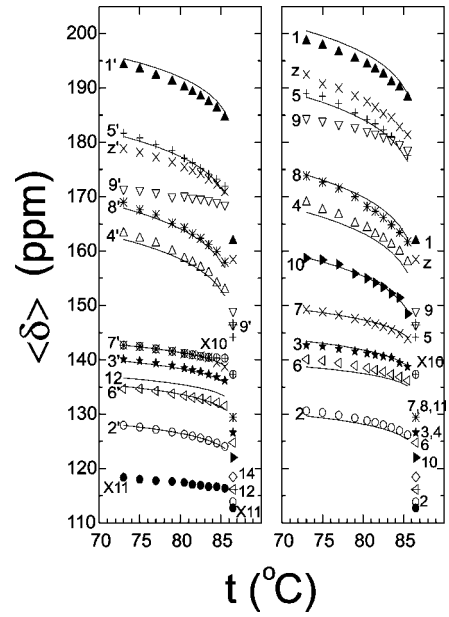

Figure 6. Plots of $\langle\delta\rangle$ for the aromatic carbons and aliphatic carbons X10 and X11 in the I and N phases of 11ClPBBC. The carbon labels are indicated in Figure 1. The unprimed labels refer to biphenyl fragment attached closer to the chlorine substituent, and the prime carbon labels refer to the other biphenyl fragment. Solid curves denote calculated $\langle\delta\rangle$ values.

tensors used in 10DClPBBC is used to analyze the $\langle\delta\rangle$ from carbons 10 and 12 of the center ring, and from carbons 1−8 of the "unprimed" and "primed" biphenyl fragments to get their local order parameters. The purpose is to see the effects, if any, of the disubstituted and monosubstituted PBBC on the overall molecular ordering and packing in their N phases.

The calculated $\langle\delta\rangle$ of the fitted carbon sites are shown as solid curves in Figure 6, and the fits are very good. The S values of center ring and two biphenyl fragments obtained from the global fit are shown in Figure 7 with S_0 and f for the center ring being (0.869, 0.142), whereas for the two bipenyl fragments they are very similar ((0.600, 0.144) for primed labels and (0.659, 0.145) for unprimed carbon labels). Again, the z-axis of the center ring is the most ordered axis. It is noted that the two para axes of the biphenyl fragments are ordered more or less the same. The β_F angles for the two biphenyl lateral wings are very close, with decreasing temperature from 24.4 to 24°, and from 27.5 to 27.3° for the umprimed and primed lateral wings. The bend angle Θ between the two lateral wings averages to ca. 128.5° and is relatively insensitive to temperature (see Figure 5). This angle is larger than that of 10DClPBBC. It is very interesting to examine the behaviors of local molecular biaxial order parameters shown in Figure 7. There is a sign change in D of the center ring between this compound and 10DClPBBC, implying different ordering of its x- and y-axes with respect to $\vec{n}$ for the two cases. For 11ClPBBC, D for the two biphenyl fragments differ in sign. This is likely a result of the monosubstitution in the center ring, causing the two lateral wings to be distinct from each other. The phenyl ring of the unprimed wing closer to the center ring appears to behave with D similar to that of the center ring. When comparing D of 10DClPBBC with those of this compound, the former has much larger absolute D values for various phenyl rings.

3.3. 10BrPBBC. The homologue 10BrPBBC[17] could only be weakly aligned very close to the I−N transition. The aligned N phase has produced a ^{13}C NMR spectrum at 69 °C. As

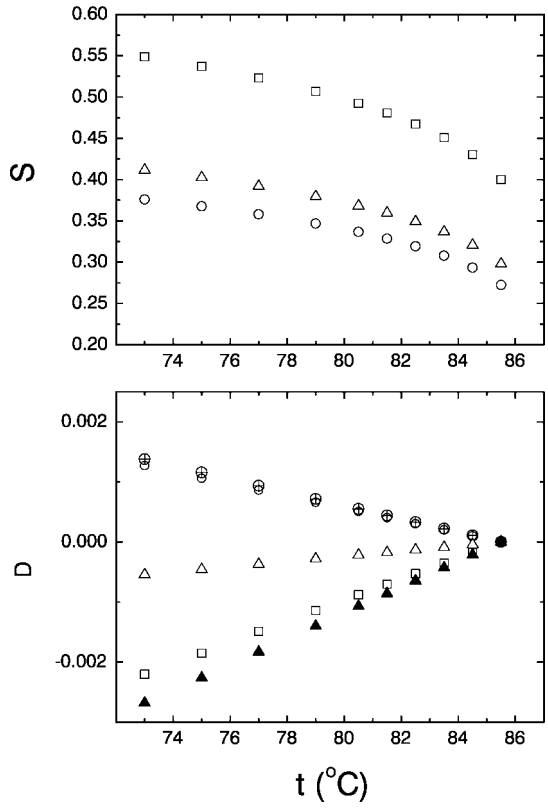

Figure 7. Top: Plot of the local order parameter *S* for the biphenyl fragments (Δ for unprimed fragment, ○ for primed fragment) and center ring (□) in the N phase of 11ClPBBC. Bottom: Plot of the local biaxial order parameter *D* vs temperature. (same symbols as for *S*, solid symbols for phenyl ring closer to the center ring, and open symbols for the outer phenyl ring in the biphenyl group).

TABLE 3: CSA Tensors for Some Carbons in 10BrPBBC from SUPER[a]

sites	1	3,6	4	5	7, 8, 11
δ_{11}	60.6	21.2	8.8	55.6	0.7
δ_{22}	159.2	136.2	131.2	140.7	151.7
δ_{33}	257.0	225.2	227.7	225.1	240.6
sites	9	10	12	13	14
δ_{11}	56.3	15.4	−7.8	58.2	5.1
δ_{22}	156.8	126.0	144.7	130.2	137.7
δ_{33}	261.7	192.3	215.5	259.8	220.9

[a] CSA components are modified by using $\delta_{ii}^{new} = (\delta_{ii} - \delta_{iso})/0.667 + \delta_{iso}$.

mentioned above, the simple replacement of bromine by chlorine in this molecule has caused a total lack of alignment in the NMR field, thus preventing any possiblity of studying ordering in this banana-shaped LC. Yet when the latter has an extra methylene group in the lateral chains, the compound could be studied as discussed above. The CSA tensors of 10BrPBBC reported in ref 17 are again corrected and listed in Table 3. These are used to interpret the ^{13}C $\langle\delta\rangle$ values for most of the carbon peaks at the only available temperature close to the I phase, and the fitted ^{13}C $\langle\delta\rangle$ values together with experimental $\langle\delta\rangle$ values are given in Table 4 for direct comparison. The *z*-axis of the central ring is still the more ordered axis with $S = 0.24$, a value that seems too low and may well indicate that the aligned N phase is metastable. Thus, any change in temperature could easily disrupt the molecular alignment, making a full study of orienational order and structure impossible.

TABLE 4: Calculated ^{13}C Chemical Shifts (δ_{cal}) for Various Sites[a]

sites	δ_{iso}	δ_{exp}	δ_{cal}	sites	δ_{iso}	δ_{exp}	δ_{cal}
1	159.0	182.4	180.5	1′	159.0	177.9	177.9
2	114.7	126.1	124.7	2′	114.7	124.1	121.9
3	127.5	136.5	136.2	3′	127.5	132.1	133.4
4	122.6	143.2	146.1	4′	122.6	142.1	142.8
5	140.5	157.5	160.2	5′	130.5	153.6	156.8
6	127.5	136.5	137.6	6′	127.5	132.1	133.5
7	131.0	143.2	144.8	7′	131.0	138.3	139.4
8	131.0	162.1	158.5	8′	131.0	155.8	152.3
9	158.3	177.9	176.4	12	117.5	124.1	124.0
10	111.2	126.1	126.4	13	149.4	167.8	167.7
11	131.0	136.5	136.1	14	121.3	138.4	139.8

[a] Measured in ppm of 10BrPBBC at 69 °C.

In summary, a twisted conformation of the bent-core can be inferred in nPBBC series from the local molecular biaxiality *D*, and the details in the orientations of ring planes depend on the substitution at the center ring. Moreover, the substitution on the center ring and the chain length have a profound effect on the alignment of the bent-core molecules by the magnetic field. The difficulty in alignment of V-shaped molecules by the magnetic field has been noted by other researchers,[24] and the reason behind this remains to be investigated. It is noted that in the studied nPPBC series the bend angle of 11ClPBBC is relatively insensitive to temperature, whereas that of 10DClPBBC decreases with lowering temperature. Thus, the choice of molecular structure in the bent-core region may ultimately determine the occurrence of a biaxial nematic phase before the crystallization set in. Recently, a new two-dimensional NMR technique called R-PDLF[25] has been successfully used under magic angle spinning to measure the C−H dipolar couplings of LC that fails to form an aligned phase. This opens an opportunity to study 10ClPBBC and 10BrPBBC to obtain ordering information. This is currently being pursued in our laboratory.

Acknowledgment. The Natural Sciences and Engineering Council of Canada is thanked for the financial support. We thank A. Marini for useful discussions.

References and Notes

(1) Niori, T.; Sekine, F.; Watanabe, J.; Furukawa, T.; Takezoe, H. *J. Mater. Chem.* **1996**, *6*, 1231.
(2) Freiser, M. J. *Phys. Rev. Lett.* **1970**, *24*, 1041.
(3) Eremin, A.; Wirth, I.; Diele, S.; Pelzl, G.; Schmalfuss, H.; Kresse, H.; Nadasi, H.; Fodor-Csorba, K.; Gacs-Baitz, E. W. *Liq. Cryst.* **2002**, *29*, 775.
(4) Dong, R. Y., *NMR of Liquid Crystals*; Springer-Verlag: New York, 1994.
(5) *NMR of Orientationally Ordered Liquids*; Burnell, E. E., de Lange, C. Eds.; Kluwer Academic: Dordrecht, 2003.
(6) Yu, L. J.; Saupe, A. *Phys. Rev. Lett.* **1980**, *45*, 1000.
(7) Madsen, L. A.; Dingemans, T. J.; Nakata, M.; Samulski, E. T. *Phys. Rev. Lett.* **2004**, *92*, 145505.
(8) Dunmur, D. A.; Toriyama, K. In *Physical Properties of Liquid Crystals*; Demus, D. Goodby, J. Gray, G. W., Spiess, H. W., Vill, V. Eds.; Wiley-VHC: Weinheim, 1999.
(9) Merkel, K.; Kocot, A.; Vij, J. K.; Korlacki, R.; Mehl, G. H.; Meyer, T. *Phys. Rev. Lett.* **2004**, *93*, 237801.
(10) Teixeira, P. I. C.; Masters, A. J.; Mulder, B. M. *Mol. Cryst. Liq. Cryst.* **1998**, *323*, 167.
(11) Luckhurst, G. R. *Thin Solid Films* **2001**, *393*, 40.
(12) Bates, M. A. *Phys. Rev. E* **2006**, *74*, 061702.
(13) Dong, R. Y.; Kumar, S.; Prasad, V.; Zhang, J. *Chem. Phys. Lett.* **2007**, *448*, 54 This preliminary report unfortunately contains errors in the chemical shift anisotropy tensors. .
(14) Dong, R. Y.; Xu, J.; Benyei, G.; Fodor-Csorba, K. *Phys. Rev. E* **2004**, *70*, 011708.

(15) Liu, S. F.; Mao, J. D.; Schmidt-Rohr, K. *J. Magn. Reson.* **2002**, *155*, 15.
(16) Xu, J.; Fodor-Csorba, K.; Dong, R. Y. *J. Phys. Chem. A* **2005**, *109*, 1998.
(17) Dong, R. Y.; Zhang, J.; Fodor-Csorba, K. *Chem. Phys. Lett.* **2006**, *417*, 475 The chemical shift anisotropy tensors reported herein unfortunately contain errors in scaling. .
(18) Dong, R. Y.; Geppi, M.; Marini, A.; Hamplova, V.; Kaspar, M.; Veracini, C. A.; Zhang, J. *J. Phys. Chem. B* **2007**, *111*, 9787.
(19) Dong, R. Y.; Xu, J.; Zhang, J.; Veracini, C. A. *Phys. Rev. E* **2005**, *72*, 061701.
(20) Allender, D. W.; Doane, J. W. *Phys. Rev. A* **1978**, *17*, 1177.
(21) Hodder, B.; Sambles, J. R.; Jenkins, S.; Richardson, R. M. *Phys. Rev. Lett.* **1999**, *85*, 3181.
(22) Catalano, D.; Cavazza, M.; Chiezzi, L.; Geppi, M.; Veracini, C. A. *Liq. Cryst.* **2000**, *27*, 621.
(23) Zheng, G.; Hu, J.; Zhang, X.; Shen, L.; Ye, C.; Webb, G. A. *J. Mol. Struct.* **1998)** , *428*, 283.
(24) Domenici, V.; Veracini, C. A.; Fofor-Csorba, K.; et al. *ChemPhysChem* **2007**, *8*, 2321.
(25) Dvinskikh, S. V.; Zimmermann, H.; Maliniak, A.; Sandstrom, D. *J. Magn. Reson.* **2004**, *168*, 194.

JP8096692